# Exact relation between Eulerian and Lagrangian velocity increment statistics

O. Kamps,[1] R. Friedrich,[1] and R. Grauer[2]
[1]*Theoretische Physik, Universität Münster, 48149 Münster, Germany*
[2]*Theoretische Physik I, Ruhr-Universität Bochum, 44780 Bochum, Germany*
(Received 10 June 2008; revised manuscript received 5 January 2009; published 3 June 2009)

We present a formal connection between Lagrangian and Eulerian velocity increment distributions which is applicable to a wide range of turbulent systems ranging from turbulence in incompressible fluids to magnetohydrodynamic turbulence. For the case of the inverse cascade regime of two-dimensional turbulence we numerically estimate the transition probabilities involved in this connection. In this context we are able to directly identify the processes leading to strongly non-Gaussian statistics for the Lagrangian velocity increments.

DOI: 10.1103/PhysRevE.79.066301 PACS number(s): 47.27.E−, 02.50.Fz, 47.10.ad

## I. INTRODUCTION

The relation between Eulerian and Lagrangian statistical quantities is a fundamental question in turbulence research. It is of crucial interest for the understanding and modeling of transport and mixing processes in a broad range of research fields spanning from cloud formation in atmospheric physics over the dispersion of microorganisms in oceans to research on combustion processes and the understanding of heat transport in fusion plasmas. The recent possibility to assess the statistics of Lagrangian velocity increments by experimental means [1,2] has stimulated investigations of relations between the Eulerian and the Lagrangian two-point velocity statistics. Especially, the emergence of intermittency (i.e., the anomalous scaling of the moments of the velocity increment distributions [3]) in both descriptions and its interrelationship is of great importance for our understanding of the spatiotemporal patterns underlying turbulence. A first attempt to relate Eulerian and Lagrangian statistics has been undertaken by Corrsin [4], who investigated Eulerian and Lagrangian velocity correlation functions. Recently, the Corrsin approximation has been reconsidered in [5], where it has become evident that it is a too crude approximation and cannot deal with the question of the connection between Eulerian and Lagrangian intermittencies. Further approaches to characterize Lagrangian velocity increment statistics are based on multifractal models [6,7] which also have been extended to the dissipation range [8]. In [7] a direct translation of the Eulerian multifractal statistics to the Lagrangian picture is presented. In this approach a nonintermittent Eulerian velocity field cannot lead to Lagrangian intermittency. This statement is in contrast with the experimental results of Rivera and Ecke [9], as well as numerical calculations performed for two-dimensional turbulence [10]. Motivated by this fact we have derived an exact relation between the Eulerian and the Lagrangian velocity increment distributions, which allows us to study the emergence of Lagrangian intermittency from a statistical point of view.

## II. CONNECTING THE INCREMENT PROBABILITY DENSITY FUNCTIONS

The quantities of interest are the Eulerian velocity increments

$$u_e = v(\boldsymbol{y}+\boldsymbol{x},t) - v(\boldsymbol{y},t), \tag{1}$$

where the velocity difference is measured at the time $t$ between two points that are separated by the distance $\boldsymbol{x}$, and the Lagrangian velocity increment

$$u_l = v(\boldsymbol{y}+\tilde{\boldsymbol{x}}(\boldsymbol{y},\tau,t),t) - v(\boldsymbol{y},t-\tau). \tag{2}$$

In the latter case the velocity difference is measured between two points connected by the distance $\tilde{\boldsymbol{x}}(\boldsymbol{y},\tau,t)$ traveled by a tracer particle during the time interval $\tau$. In both cases $v$ is defined as the projection $\boldsymbol{v}\cdot\hat{\boldsymbol{e}}_i$ of the velocity vector on one of the axes ($i=x,y,z$ in three dimensions and $i=x,y$ in two dimensions) of the coordinate system (see, e.g., [11,12]). In the case of an isotropic flow the results do not depend on the chosen axis; however, we do not have to make this assumption yet. Additionally, we define the velocity increment

$$u_{el} = v(\boldsymbol{y}+\tilde{\boldsymbol{x}}(\boldsymbol{y},\tau,t),t) - v(\boldsymbol{y},t), \tag{3}$$

which is a mixed Eulerian-Lagrangian quantity because the points are separated by $\tilde{\boldsymbol{x}}$ but the velocities are measured at the same time. The properties of this quantity have been investigated in [13]. Finally, we introduce

$$u_p = v(\boldsymbol{y},t) - v(\boldsymbol{y},t-\tau), \tag{4}$$

measuring the velocity difference over the time $\tau$ at the starting point of the tracer. Following [14,15] we define the so-called fine-grained probability density function (PDF) for $u_e$ as

$$\hat{f}_e(v_e;\boldsymbol{x},\boldsymbol{y},t) = \delta(u_e - v_e), \tag{5}$$

where $u_e$ is the random variable and $v_e$ is the independent sample-space variable. The fine-grained PDF describes the elementary event of finding the value $v_e$ given the measured $u_e = v(\boldsymbol{y}+\boldsymbol{x},t) - v(\boldsymbol{y},t)$. The relation to the PDF is determined by

$$f_e(v_e;\boldsymbol{x},\boldsymbol{y},t) = \langle \hat{f}_e(v_e;\boldsymbol{x},\boldsymbol{y},t)\rangle, \tag{6}$$

where the angular brackets denote ensemble averaging. The quantity $f_e$ is a function with respect to the variables $\boldsymbol{x},\boldsymbol{y},t$ and a PDF with respect to the variable $v_e$. In analogy to Eq. (5) we can define fine-grained PDFs for all other quantities. Now we want to derive an exact relation between the fine-

 

grained PDFs $\hat{f}_e$ and $\hat{f}_l$. This task can be split up into two steps. First we have to replace the distance $\boldsymbol{x}$ with the trajectory $\tilde{\boldsymbol{x}}(\boldsymbol{y},\tau,t)$ of a tracer in order to translate from $u_e$ to $u_{el}$. This is done by

$$\hat{f}_{el}(v_e;\boldsymbol{y},\tau,t) = \int d\boldsymbol{x}\ \delta(\tilde{\boldsymbol{x}}(\boldsymbol{y},\tau,t)-\boldsymbol{x})\hat{f}_e(v_e;\boldsymbol{x},\boldsymbol{y},t). \quad (7)$$

We see that during this operation the sample-space variable is not affected. The subscript in $\hat{f}_{el}$ denotes the fact that we now have $v_e=u_{el}$ instead of $v_e=u_e$. In the second step we have to connect $\hat{f}_l$ and $\hat{f}_{el}$. From the definitions of increments (2)–(4) we see that $u_l=u_{el}+u_p$ and therefore the fine-grained PDF for $u_l$ is given by the fine-grained distribution of the sum of $u_{el}$ and $u_p$. To that end we have to multiply $\hat{f}_{el}(v_e;\boldsymbol{y},\tau,t)$ with $\hat{f}_{el}(v_e;\boldsymbol{y},\tau,t)=\delta(u_p-v_p)$ to get the fine-grained joint probability of finding $u_{el}$ and $u_p$ at the same time. Subsequent application of $\int dv_e \int dv_p\ \delta[v_l-(v_e+v_p)]$ leads to

$$\hat{f}_l(v_l;\boldsymbol{y},\tau,t) = \int dv_e\, \hat{f}_p(v_l-v_e;\boldsymbol{y},\tau,t)\hat{f}_{el}(v_e;\boldsymbol{y},\tau,t). \quad (8)$$

To derive the corresponding PDFs we have to perform the ensemble average. In the case of Eq. (8) we obtain

$$f_l(v_l;\boldsymbol{y},\tau,t) = \left\langle \int dv_e\, \hat{f}_p(v_l-v_e;\boldsymbol{y},\tau,t)\hat{f}_{el}(v_e;\boldsymbol{y},\tau,t) \right\rangle$$
$$= \int dv_e\, f_p(v_l-v_e|v_e;\boldsymbol{y},\tau,t) f_{el}(v_e;\boldsymbol{y},\tau,t). \quad (9)$$

In the last line we used the general relation $p(a,b)=p(a|b)p(b)$ valid for two random variables in order to extract $f_{el}$ from the average. We can treat Eq. (7) in a similar manner. This leads us to

$$f_{el}(v_e;\boldsymbol{y},\tau,t) = \left\langle \int d\boldsymbol{x}\ \delta(\tilde{\boldsymbol{x}}(\boldsymbol{y},\tau,t)-\boldsymbol{x})\hat{f}_e(v_e;\boldsymbol{x},\boldsymbol{y},t) \right\rangle$$
$$= \int d\boldsymbol{x}\langle \delta(\tilde{\boldsymbol{x}}(\boldsymbol{y},\tau,t)-\boldsymbol{x})|v_e\rangle \hat{f}_e(v_e;\boldsymbol{x},\boldsymbol{y},t). \quad (10)$$

Inserting Eq. (9) into Eq. (10) shows that the Eulerian and the Lagrangian velocity increment PDFs are connected via the transition probabilities $p_a=\langle \delta(\tilde{\boldsymbol{x}}(\boldsymbol{y},\tau,t)-\boldsymbol{x})|v_e\rangle$ and $p_b=f_p(v_l-v_e|v_e;\boldsymbol{y},\tau,t)=f_p(v_p|v_e;\boldsymbol{y},\tau,t)$. Before we connect both equations we introduce some simplifications. In most experiments and numerical simulations dealing with Lagrangian statistics, the flow is assumed to be stationary and homogeneous. In this case we may average with respect to $\boldsymbol{y}$ and $t$ and hence the dependence on this parameter in Eqs. (9) and (10) drops. Under the assumption of isotropy $f_{el}$ depends only on $r=|\boldsymbol{x}|$. Therefore, we can introduce spherical coordinates in Eq. (10) and integrate with respect to the angles. As mentioned before, in the case of isotropy the statistical quantities do not depend on the chosen axis. Finally, we arrive at

$$f_l(v_l;\tau) = \int dv_e\, p_b(v_l-v_e|v_e;\tau) \underbrace{\int_0^\infty dr\, p_a(r|v_e;\tau) f_e(v_e;r)}_{f_{el}(v_e;\tau)}. \quad (11)$$

For convenience, we included the integrated functional determinant ($2\pi r$ in two and $4\pi r^2$ in three dimensions) in $p_a$. In this case $p_a(r|v_e;\tau)$ is a measure for the turbulent transport and gives the probability of finding a tracer traveling the absolute distance $r$ within the time interval $\tau$. Multiplication by $f_e(v_e;r)$ and subsequent integration over the whole $r$ range mix the Eulerian statistics from different length scales $r$ weighted by $p_a$ to form the PDF $f_{el}(v_e;\tau)$ for a fixed time delay $\tau$. The occurrence of the condition in $p_a$ shows that this weighing depends on $u_e$. The transition probability $p_b$ incorporates the fact that during the motion of the tracer particle the velocity at the starting point changes by $u_p$. Multiplying $f_{el}(v_e;\tau)$ with $p_b$ and integrating over $v_e$ sort all events where $u_{el}+u_p=u_l$ into the corresponding bin of the histogram for $u_l$. We want to stress that Eqs. (9) and (10) and except from symmetry considerations also Eq. (11) are of a purely statistical nature and, as a consequence, hold for quite different turbulent fields. They are valid for two-dimensional as well as three-dimensional incompressible turbulence but can also be applied to magnetohydrodynamic turbulence. The differences in the details of these turbulent systems, which are connected to the presence of different types of coherent structures like localized vortices in the case of incompressible fluid turbulence or sheetlike structures in magnetohydrodynamic turbulence, are therefore closely related to the functional form of $p_a$ and $p_b$.

## III. TWO-DIMENSIONAL TURBULENCE

In this section we want to estimate numerically the two transition PDFs in Eq. (11) for the case of the inverse energy cascade of two-dimensional turbulence. The data are taken from a pseudospectral simulation of the inverse energy cascade in a periodic box with box length of $2\pi$ [10]. Recapitulating the derivation of Eq. (11) we see that we need the velocity at the start and the end points of a tracer trajectory at the same time to estimate the transition PDFs. Therefore we have to record the velocity at the starting points of the tracers additionally to their current position and their current velocity. In Fig. 1 the transition probabilities $p_a$ and $p_b$ are depicted for $\tau=0.09T_I$, where $T_I$ denotes the Lagrangian integral time scale [16]. We have chosen this rather small time lag as an example because in this case the deviation of the Lagrangian increment PDF from a Gaussian is significant. The transition probability $p_a$ can be approximated by

$$p_a(r|v_e;\tau) = N(v_e,\tau) r \exp\{-[r-m(v_e,\tau)]^2/\sigma^2(v_e,\tau)\}. \quad (12)$$

For small $v_e$ we have $m(v_e,\tau)\sim\alpha(\tau)|v_e|$ and $\sigma^2(v_e,\tau)\sim\beta(\tau)$. From the functional form of $p_a$ one can see that the transport of the tracer particles is of probabilistic nature. For any fixed $v_e$ the tracers travel different distances during the same time $\tau$. We also see a strong dependence on the condition $v_e$ which can be interpreted as the deterministic part of

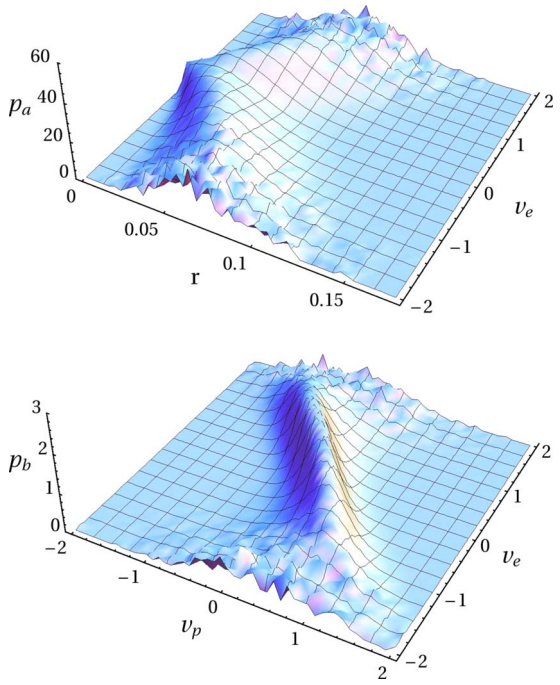


FIG. 1. (Color online) The plot shows $p_a(r|v_e;\tau)$ (top) and $p_a(v_p|v_e;\tau)$ (bottom) for $\tau=0.09T_I$.

the turbulent transport. This distinguishes it from pure diffusion and directly shows that the widely used Corrsin approximation is violated. In the case of deterministic transport $p_a$ would be proportional to $\delta(r-m(v_e,\tau))$. A good approximation for $p_b$ is given by

$$p_b(v_p|v_e;\tau)=N(v_e,\tau)\exp\{-[u_p-m(v_e,\tau)]^2/\sigma^2(v_e,\tau)\} \tag{13}$$

with $m(v_e,\tau)=\alpha(\tau)\tanh[\beta(\tau)v_e]$ and $\sigma^2(v_e,\tau)=\gamma(\tau)\times[1+\delta(\tau)|v_e|]$. For small $v_e$ we see a strong negative correlation between $v_e$ and $v_p$ [here $\tanh(v_e)\sim v_e$]. Both quantities tend to cancel in this case. This negative correlation between the sample-space variables in $p_b$ is connected with the sweeping effect. For a tracer starting with $v_1$ traveling at the time $\tau$ without changing its velocity, we have $u_{el}=v_1-v_2$ when the velocity at the starting point changes during $\tau$ from $v_1$ to $v_2$. In this case we have $u_p=v_2-v_1=-u_{el}$. This corresponds to an idealized situation but it gives a hint at the cause of the negative correlations in $p_b$. For larger $v_e$ the correlation decreases. This is captured by the fact that $\tanh[\beta(\tau)v_e]\sim$ const for large $v_e$. For both transition PDFs we observe that for increasing $\tau$ the dependence on their conditions vanishes.

Now we want to turn to the question of how the transition PDFs transform the Eulerian PDF $f_e(v_e;r)$ into the Lagrangian PDF $f_l(u_l;\tau)$. This process is depicted in Fig. 2. The left part of the figure shows several examples of $f_e(v_e;r)$. Applying $\int dr\, p_a(r|v_e;\tau)$ [see Eq. (11)] superposes different Eulerian PDFs $f_e(v_e;r)$ with different variances leading to the triangular shape in the semilogarithmic plot of the new PDF $f_{el}(v_e;\tau)$ (middle of Fig. 2). During the transition from $f_{el}(v_e;\tau)$ to $f_l(v_l;\tau)$ the variables $v_p$ and $v_e$ are added to form $v_l$. The previously described observation that $v_p$ and $v_e$ tend to cancel each other for small $v_e$ leads to a stronger weighting of very small $v_l$, so that the new PDF $f_l(v_l;\tau)$ is strongly peaked around zero (right part of Fig. 2). In contrast to the center of the distribution the tails seem not to be influenced significantly by $p_b(v_p|v_e;\tau)$. This is in agreement with the fact that for large $v_e$ the correlation between $v_e$ and $v_l$ decreases.

## IV. THREE-DIMENSIONAL TURBULENCE

To get an impression of the transition probabilities in three-dimensional turbulence we used the data provided by [7,17] to calculate the PDF $p_a(r;\tau)$ for different $\tau$. The result is depicted in Fig. 3. We see that, as in the two-dimensional case, the Lagrangian time scale $\tau$ is related to the Eulerian length scales by a PDF. This well-known result shows that in principle it is not possible to connect them by a Kolmogorov-type relation such as $\tau\sim r/\delta u_r$ [7]. In this relation $\tau$ is a typical eddy turnover time connected to eddies of length scale $r$.

In our example we have chosen three different values of the time delay $\tau$ taken from the inertial range. Even when the maximum of $p_a$ is at a distance $r$, which lies in the Eulerian inertial range, there are significant contributions from very small and very large $r$. From this observation we can conclude that due to the turbulent transport the Lagrangian statistics is influenced by contributions from the Eulerian integral and dissipative length scales.

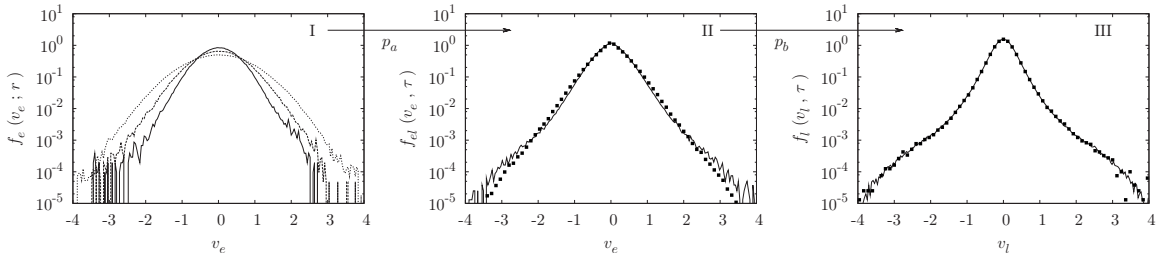


FIG. 2. The figure shows the impact of the transition probabilities on the Eulerian PDF. The left part of the figure shows $f_e(v_e;r)$ for $r=0.06,0.12,0.3$. These PDFs are transformed into $f(v_e;\tau)$ (middle) by the transition PDF presented in the upper half of Fig. 1. Subsequently $f(v_e;\tau)$ is converted into $f_l(v_l;\tau)$ (right picture) by the second transition PDF from Fig. 1. In both cases $\tau=0.09T_I$. In plots II and III the points denote the reconstructed PDFs based on Eqs. (9) and (10), and the lines denote the PDFs directly computed from the Lagrangian data.

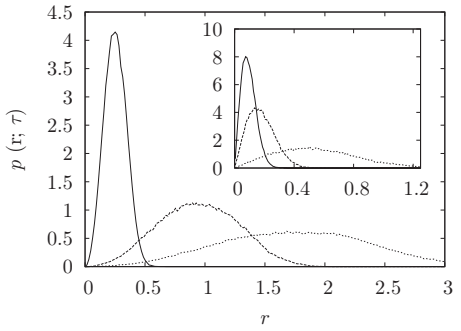


FIG. 3. The figure shows $p_a(r;\tau)$ for $\tau=3.5\tau_\eta, 14\tau_\eta, 28\tau_\eta$ for three-dimensional turbulence. In the inset $p_a$ is depicted for the two-dimensional case with $\tau=0.22T_l, 0.44T_l, 0.9T_l$.

## V. RELATION TO THE MULTIFRACTAL APPROACH

The characterization of the relation between Eulerian and Lagrangian PDFs with the help of the conditional probabilities $p_a(r|v_e;\tau)$ (Eulerian to semi-Lagrangian transition) and $p_b(v_p|v_e;\tau)$ (semi-Lagrangian to Lagrangian transition) allows one to recover a well-known multifractal approach for relating Eulerian and Lagrangian structure function exponents [7]. As a side product, a simpler formula for the Lagrangian structure function exponents of this multifractal approach will be obtained. Regarding the translation rule in [7] we would have a fixed relationship $|\vec{x}| \sim v_e\tau$ ($\delta u_r$ corresponds to $u_e$ in our notation) between the time lag $\tau$ and the distance traveled by a tracer particle during this time. This would correspond to choosing $p_a \sim \delta(r-v_e\tau)$ in Eq. (11). The additional assumption [7] $\delta v_\tau \sim \delta u_r$ ($u_l \sim u_e$ in our notation) that the velocity fluctuations on the time scale $\tau$ are proportional to the fluctuations on the length scale $r$ could be incorporated in our framework by choosing $p_b \sim \delta(v_l - v_e)$ leading to

$$f_l(v_l;\tau) = \int dv_e\ \delta(v_l - v_e) \int_0^\infty dr\ \delta(r - v_e\tau) f_e(v_e;r) = f_e(v_l;v_l\tau). \tag{14}$$

The exponents for the Lagrangian structure function exponents can now be obtained by making use of the Mellin transform

$$f_e(v_e,r) = \frac{1}{v_e}\int_{-i\infty}^{i\infty} dn\ S_e(n) v_e^{-n} \tag{15}$$

with $S_e(n)=A_e(n)r^{\zeta_e(n)}$. Here, we use the same notation as in [18]. Please note that it will not be necessary to know the amplitudes $A_e(n)$ but only the Eulerian scaling exponents $\zeta_e(n)$. Using Eq. (14) and the Mellin transform we obtain

$$f_l(v_l;\tau) = \frac{1}{v_l}\int_{-i\infty}^{i\infty} dn\ A_e(n)\tau^{\zeta_e(n)} v_l^{\zeta_e(n)-n}. \tag{16}$$

This Lagrangian PDF is now inserted into the inverse Mellin transform to obtain the Lagrangian structure functions

$$S_l(n) = \int_0^\infty dv_l\ v_l^n f_l(v_l;\tau) = \int_0^\infty dv_l \frac{1}{v_l} v_l^n \int_{-i\infty}^{i\infty} dj\ A_e(j)\tau^{\zeta_e(j)} v_l^{\zeta_e(j)-j}. \tag{17}$$

Now we substitute $j'(j)=j-\zeta_e(j)$, $dj'=[1-\partial_j\zeta_e(j)]dj$, and denote the inverse function by $j=j(j')$. Thus we have

$$S_l(n) = \int_0^\infty dv_l \frac{1}{\delta v_l} v_l^n \int_{-i\infty}^{i\infty} dj'\ S_l(j')(\delta v_l)^{-j'} \tag{18}$$

with $S_l(j') = \frac{A_e(j)}{1-\partial_j\zeta_e(j)}\tau^{\zeta_e(j)}$ and $j'=j-\zeta_e(j)$, and we obtain for the exponents

$$\zeta_l[n-\zeta_E(n)] = \zeta_e(n) \tag{19}$$

It remains to show that this relation (19) is identical to the formulas derived by Biferale *et al.* [7]. To see this, we shortly repeat the multrifractal approach which starts with the Eulerian structure function exponents

$$\zeta_e(p) = \inf_h[ph + 3 - D_e(h)] = ph_e^* + 3 - D_e(h_e^*) \tag{20}$$

and $p=D_e'(h_e^*)$. Here $D_e(h)$ is the Eulerian singularity spectrum and $h_e^*$ is the value where the infimum is achieved. The assumption $r=v_e\tau$ appears now in the denominator of the expression of the Lagrangian structure function exponents

$$\zeta_l(p) = \inf_h\left(\frac{ph + 3 - D_e(h)}{1-h}\right). \tag{21}$$

From this it follows

$$\zeta_l[p-\zeta_e(p)] = \inf_h\left(\frac{[p-ph_e^* - 3 + D_e(h_e^*)]h + 3 - D_e(h)}{1-h}\right). \tag{22}$$

In order to find the infimum we differentiate with respect to $h$,

$$D_e'(h_e^*) - D_e'(h) + D_e(h_e^*) - D_e(h) - D_e'(h_e^*)h_e^* + D_e'(h)h \stackrel{!}{=} 0. \tag{23}$$

From this it follows that $h_L^*=h_E^*$ and

$$\zeta_L(p-\zeta_e(p)) = ph_e^* + 3 - D_e(h_e^*) = \zeta_e(p), \tag{24}$$

which recovers Eq. (19). A consequence of Eqs. (14) and (19) is that for a self-similar Eulerian velocity field (as we can find it in the two-dimensional inverse energy cascade) we should find self-similar Lagrangian PDFs. As mentioned above this is in contradiction to recent experiments [9] and our own numerical simulations [10].

## VI. CONCLUSION AND OUTLOOK

We presented a straightforward derivation of an exact relationship between Eulerian and Lagrangian velocity increment PDFs. For the example of two-dimensional forced turbulence we were able to explain how it is possible to observe

strongly non-Gaussian intermittent distributions for the Lagrangian velocity increments. The two mechanisms in this context are the turbulent transport of the tracers leading to the mixing of statistics from different length scales and the velocity change at the starting point of the tracers leading to a further deformation of the increment PDF. In comparison we analyzed data from simulations of three-dimensional turbulence. Similar to the two-dimensional case we demonstrated that Lagrangian time and Eulerian length scales are connected via a transition PDF that varies with the time scale. We were also able to show that the well-known multifractal model for the Lagrangian structure functions is a limiting case of the presented translation rule. The next step is to estimate the transition probabilities for three-dimensional turbulence as well as magnetohydrodynamic turbulence in order to get a deeper understanding of the influence of the underlying physical mechanisms, especially the presence of coherent structures on the translation process. In this context the question of why intermittency in the Lagrangian picture is stronger in magnetohydrodynamics than in fluid turbulence [19], although the situation is reversed in the Eulerian picture, will be addressed.

## ACKNOWLEDGMENTS

We are grateful to H. Homann, M. Wilczek, and D. Kleinhans for fruitful discussions and we acknowledge support from the Deutsche Forschungsgesellschaft (Grants No. FR 1003/8-1 and No. FG 1048). We also thank the supercomputing center Cineca (Bologna, Italy) for providing and hosting the data for 3D turbulence.

[1] A. La Porta, G. Voth, A. M. Crawford, J. Alexander, and E. Bodenschatz, Nature (London) **409**, 1017 (2001).
[2] N. Mordant, P. Metz, O. Michel, and J.-F. Pinton, Phys. Rev. Lett. **87**, 214501 (2001).
[3] U. Frisch, *Turbulence: The Legacy of A. N. Kolmogorov* (Cambridge University Press, Cambridge, England, 1995).
[4] S. Corrsin, in *Advances in Geophysics*, edited by F. N. Freinkel and P. A. Sheppard (Academic, New York, 1959), Vol. 6, p. 161.
[5] S. Ott and J. Mann, J. Fluid Mech. **422**, 207 (2000).
[6] M. S. Borgas, Philos. Trans. R. Soc. London, Ser. A **342**, 379 (1993).
[7] L. Biferale, G. Boffetta, A. Celani, B. J. Devenish, A. Lanotte, and F. Toschi, Phys. Rev. Lett. **93**, 064502 (2004).
[8] L. Chevillard, S. G. Roux, E. Leveque, N. Mordant, J. F. Pinton, and A. Arneodo, Phys. Rev. Lett. **91**, 214502 (2003).
[9] M. K. Rivera and R. E. Ecke, e-print arXiv:0710.5888.
[10] O. Kamps and R. Friedrich, Phys. Rev. E **78**, 036321 (2008).
[11] N. Mordant, E. Lévêque, and J.-F. Pinton, New J. Phys. **6**, 116 (2004).
[12] G. Voth, A. L. Porta, A. Crawford, J. Alexander, and E. Bodenschatz, J. Fluid Mech. **469**, 121 (2002).
[13] R. Friedrich, R. Grauer, H. Homann, and O. Kamps, Phys. Scr. **79**, 055403 (2009).
[14] T. S. Lundgren, Phys. Fluids **10**, 969 (1967).
[15] S. B. Pope, *Turbulent Flows* (Cambridge University Press, Cambridge, England, 2000).
[16] P. K. Yeung, Annu. Rev. Fluid Mech. **34**, 115 (2002).
[17] L. Biferale, G. Boffetta, A. Celani, A. Lanotte, and F. Toschi, Phys. Fluids **17**, 021701 (2005).
[18] V. Yakhot, Physica D **215**, 166 (2006).
[19] H. Homann, R. Grauer, A. Busse, and W. C. Müller, J. Plasma Phys. **73**, 821 (2007).